

Tobias Nilsson, Benedikt Soja, Kyriakos Balidakis, Maria Karbon, Robert Heinkelmann, Zhiguo Deng, Harald Schuh

Improving the modeling of the atmospheric delay in the data analysis of the Intensive VLBI sessions and the impact on the UT1 estimates

Journal article | Accepted manuscript (Postprint)

This version is available at <https://doi.org/10.14279/depositonce-11880>



This is a post-peer-review, pre-copyedit version of an article published in Journal of Geodesy. The final authenticated version is available online at: <http://dx.doi.org/10.1007/s00190-016-0985-7>

Nilsson, T., Soja, B., Balidakis, K., Karbon, M., Heinkelmann, R., Deng, Z., & Schuh, H. (2017). Improving the modeling of the atmospheric delay in the data analysis of the Intensive VLBI sessions and the impact on the UT1 estimates. *Journal of Geodesy*, 91(7), 857–866. <https://doi.org/10.1007/s00190-016-0985-7>

Terms of Use

Copyright applies. A non-exclusive, non-transferable and limited right to use is granted. This document is intended solely for personal, non-commercial use.

WISSEN IM ZENTRUM
UNIVERSITÄTSBIBLIOTHEK

Technische
Universität
Berlin

1 **Improving the modeling of the atmospheric delay in**
2 **the data analysis of the Intensive VLBI sessions and**
3 **the impact on the UT1 estimates**

4 **Tobias Nilsson · Benedikt Soja · Kyriakos**

5 **Balidakis · Maria Karbon · Robert**

6 **Heinkelmann · Zhiguo Deng · Harald**

7 **Schuh**

8 Received: date / Accepted: date

This work was supported by the Austrian Science Fund (FWF), project number P24187-N21
(VLBI-ART).

T. Nilsson · B. Soja · M. Karbon · R. Heinkelmann · Z. Deng · H. Schuh

Department 1: Geodesy and Remote Sensing

Helmholtz Centre Potsdam

GFZ German Research Centre for Geosciences

14473 Potsdam, Germany

Tel.: +49 331-288-1144

Fax: +49 331-288-1111

E-mail: nilsson@gfz-potsdam.de

K. Balidakis · H. Schuh

Technische Universität Berlin

Institute of Geodesy and Geoinformation Science

Straße des 17. Juni 135

10623 Berlin, Germany

9 **Abstract** The VLBI (very long baseline interferometry) Intensive sessions are
10 typically 1-hour and single-baseline VLBI sessions, specifically designed to yield
11 low-latency estimates of UT1-UTC. In this work, we investigate what accuracy is
12 obtained from these sessions and how it can be improved. In particular, we study
13 the modeling of the troposphere in the data analysis. The impact of including
14 external information on the zenith wet delays (ZWD) and tropospheric gradients
15 from GPS or numerical weather prediction models is studied. Additionally, we test
16 estimating tropospheric gradients in the data analysis, which is normally not done.
17 To evaluate the results we compared the UT1-UTC values from the Intensives to
18 those from simultaneous 24-h VLBI session. Furthermore, we calculated Length
19 of Day (LOD) estimates using the UT1-UTC values from consecutive Intensives
20 and compared these to the LOD estimated by GPS. We find that there is not
21 much benefit in using external ZWD, however, including external information on
22 the gradients improves the agreement with the reference data. If gradients are
23 estimated in the data analysis, and appropriate constraints are applied, the WRMS
24 difference w.r.t. UT1-UTC from 24-h sessions is reduced by 5 % and the WRMS
25 difference w.r.t. the LOD from GPS by up to 12 %. The best agreement between
26 Intensives and the reference time series are obtained when using both external
27 gradients from GPS and additionally estimating gradients in the data analysis.

28 **Keywords** VLBI, Intensives, Universal time 1, Length of day, Kalman filter,
29 Troposphere, Tropospheric gradients

1 Introduction

Very long baseline interferometry (VLBI) is one of the main techniques for measuring the Earth orientation parameters (EOPs). In particular, VLBI is the only technique capable of determining Universal Time (UT1-UTC) and precision/nutation. Coordinated by the International VLBI Service for Geodesy and Astrometry (IVS, Schuh and Behrend, 2012), two so-called rapid turnaround (IVS-R1 and IVS-R4) 24-h VLBI sessions are observed every week, with the main purpose being to estimate the EOPs. For logistic reasons, the results from these sessions are typically available with a latency of about two weeks. It is, however, for many applications desirable to have the results available with lower latency and with higher time resolution. In order to provide this for UT1-UTC, special 1-hour VLBI sessions, so-called Intensives (Robertson et al., 1985), are observed every day. Typically these sessions are observed with just two stations on a long East-West baseline (needed to have good sensitivity to UT1-UTC). The results are typically available within two days.

Currently, mainly three different types of Intensives are observed within the IVS, see Fig. 1. On weekdays, between 18:30 UT and 19:30 UT, the INT1 sessions are observed with the stations Wettzell (Germany) and Kokee Park (Hawaii, USA). Sometimes, also the station Svetloe (Russia) participates in these sessions. On weekends, between 07:30 UT and 08:30 UT, the INT2 sessions are observed with Wettzell and Tsukuba (Japan). Additionally, the INT3 sessions are observed on Mondays between 07:00 UT and 08:00 UT, using the three stations Wettzell, Tsukuba, and Ny-Ålesund (Spitsbergen, Norway) (Luzum and Nothnagel, 2010). Occasionally, when one of the original stations used in the Intensives has been un-

54 available due to, e.g. a repair of the antenna, another station has been used instead.
55 Additionally, there are a few Intensives series observed outside the framework of
56 the IVS, i.e. in Russia and the USA. In this paper, we only investigate the IVS
57 Intensives and, unless otherwise noted, we will for consistency use the designation
58 INT1 to denote only those Intensives observed with the baseline Wettzell–Kokee
59 and INT2 to denote only the sessions observed with Wettzell–Tsukuba.

60 The accuracy of the results obtained from the Intensives are, however, limited
61 for a number of reasons. First of all, since typically the observations are made
62 with just a single baseline and the sessions are just 1 hour long, it is impossible
63 to use the same parametrization of the Earth orientation as in the processing a
64 standard 24-h VLBI session (offsets for all five EOP, and rates for polar motion and
65 UT1-UTC), without imposing strong constraints. In principle, it is only possible
66 to estimate two parameters describing the orientation since the observations are
67 insensitive to any rotation around the baseline and 1 hour is too short to properly
68 separate polar motion and precession/nutation. Secondly, since the sessions are
69 only one hour long, the number of observations are limited. Normally, only 20–
70 40 observations are made in an Intensive (about 20 in an INT1 session and 30–40
71 in an INT2). Furthermore, the geometrical distribution of the radio sources is not
72 optimal since a very long baseline (8000–10000 km) is used, and the radio sources
73 need to be visible from both stations. Because of these reasons, the number of
74 parameters that can be estimated in the data analysis of an Intensive session is
75 limited. Typically, only one clock polynomial (offset, rate, and sometimes also a
76 quadratic term), one constant zenith wet delay (ZWD) per station, as well as one
77 UT1-UTC offset are estimated. Other parameters, such as polar motion, celestial
78 pole offsets, station coordinates, and tropospheric gradients, are fixed to their a

79 priori values. Thus, any unmodeled errors in these a priori values could cause errors
 80 in the estimates of UT1-UTC (and other parameters).

81 Since the Intensives is the only source of low-latency UT1-UTC currently ex-
 82 isting, there is a desire to improve the accuracy. This is important for all appli-
 83 cations needing low-latency UT1-UTC information, e.g. satellite and space craft
 84 navigation. In several works different ways of improving the accuracy have been
 85 investigated. For example, Gipson and Baver (2016) investigated the effect of ap-
 86 plying two different strategies when scheduling the sessions, Nothnagel and Schnell
 87 (2008) and Malkin (2011) investigate the effect of the a priori polar motion and ce-
 88 lestial pole offsets used in the data analysis, and Malkin (2013) studied the impact
 89 of neglecting the seasonal station motions in the data analysis.

90 The neutral atmosphere is one of the largest error sources for geodetic VLBI
 91 (Nilsson and Haas, 2010). Normally, the atmospheric delay, ℓ_{atm} , is modeled in
 92 the VLBI data analysis by the following expression (e.g., Nilsson et al., 2013):

$$\ell_{atm} = m_h(\epsilon) \ell_h^z + m_w(\epsilon) \ell_w^z + m_g(\epsilon) [G_n \cos a + G_e \sin a] \quad (1)$$

93 where ℓ_h^z and ℓ_w^z denote the zenith hydrostatic delay (ZHD) and ZWD, respec-
 94 tively, m_h and m_w are the hydrostatic and wet mapping functions, respectively
 95 (e.g., Böhm et al., 2006), m_g is the gradient mapping function (e.g., Chen and
 96 Herring, 1997), G_n and G_e are the tropospheric gradients in the north and east
 97 directions, respectively, ϵ is the elevation angle, and a the azimuth angle of the
 98 observation. The first two terms on the right-hand side of Eq. (1) describe the a
 99 part of the atmospheric delay independent of the azimuth angle, while azimuthal
 100 dependence is taken into account by the third term (to the first order approx-
 101 imation). More specifically, the third term describes the delay caused by linear

horizontal variations in the refractive index above the site, or, equivalently, by tilting of the mapping function (see e.g. Nilsson et al. 2013 for details). The ZHD can be accurately determined from surface pressure measurements (Davis et al., 1985), and accurate expressions for the mapping functions exist. However, due to the fact that water vapor is highly volatile in both space and time accurate values of the ZWD, as well as G_n and G_e , are not easily obtainable, hence these are typically estimated (as piece-wise linear functions) in the data analysis of standard 24-h VLBI sessions. In the data analysis of Intensives, however, only the ZWD (as a constant value over the whole session) is estimated while the gradients are normally fixed to the prediction of a simple empirical model (or even to zero). Such empirical models can induce significant errors since they do not model the rapid variations in the gradients on timescales from hours to days, but normally only the climatological mean over several years. This will propagate into errors of the parameters estimated in the data analysis, such as UT1-UTC. For example, if there is a common error in the a priori East gradient of 1 mm, which is not unrealistic, this will cause a UT1-UTC error of 20–30 μas (Nilsson et al., 2011, 2014).

Böhm et al. (2010) performed tests using ray-traced delays, as well as a priori gradients calculated from ECMWF data, in the analysis of the INT2 sessions. They compared the Length of Day (LOD) estimated from consecutive Intensives with the estimates from a GNSS (Global Navigation Satellite Systems) solution. A slight improvement was found using the ray-traced delays, but no improvement when using ECMWF gradients. Teke et al. (2015) used gradients and ZWD estimated from GNSS data in the analysis of the Intensive sessions and found an improvement in the agreement between LOD estimated from sequential Intensives and those

127 estimated from GNSS when doing so. Another approach for handling the gradients
128 is to estimate them in the data analysis, as suggested by Nilsson et al. (2011).
129 This is possible if they are tightly constrained to their a priori values. As shown
130 by Nilsson et al. (2011) and Nilsson et al. (2014) this can improve the agreement
131 of UT1-UTC estimated from the Intensives with those estimated from 24-h VLBI
132 sessions.

133 In this work, we investigate the accuracy of the UT1-UTC estimates from
134 the Intensives and ways to improve it. In particular, we focus on how to handle
135 the errors introduced by the atmosphere. We further evaluate the possibility of
136 estimating gradients in the data analysis and derive the optimal levels of the con-
137 straints needed to be applied to these. Furthermore, we study the possibility to use
138 tropospheric gradients and ZWD from GPS. Here, we do not only test the effect
139 of using the GPS estimates as a priori values, but also the possibility to include
140 them as additional observations in the data analysis. We apply two methods of
141 validating the results. The first is a direct comparison with the UT1-UTC esti-
142 mated from simultaneous 24-h VLBI sessions. The second method is an indirect
143 validation of the UT1-UTC estimates from the Intensives by first estimating the
144 LOD using UT1-UTC from two consecutive Intensive sessions and then comparing
145 these values to with the LOD values estimated from GPS.

146 **2 Data analysis**

147 We have analyzed all Intensive sessions from the period 2002–2015, in total 4428 ses-
148 sions, with the GFZ version of the Vienna VLBI Software (Böhm et al., 2012),
149 VieVS@GFZ (Nilsson et al., 2015; Soja et al., 2015). The a priori modeling ba-

150 sically follows the IERS 2010 Conventions (Petit and Luzum, 2010), except that
151 we also corrected for non-tidal atmospheric loading (Petrov and Boy, 2004). For
152 the modeling of the atmospheric delays we applied the Vienna Mapping Functions
153 (VMF1, Böhm et al., 2006) and the gradient mapping function of Chen and Her-
154 ring (1997). The a priori gradients were obtained from the static a priori gradient
155 (APG) model (Böhm et al., 2013), which provides the climatological mean gradi-
156 ent based on ECMWF operational analysis data. The a priori station and radio
157 source coordinates were taken from the ITRF2014¹ and ICRF2 (Fey et al., 2015)
158 catalogs, respectively, while the a priori EOP were taken from the USNO finals
159 series².

160 For the parameter estimation, we used the Kalman filter module of VieVS@GFZ,
161 VIE_KAL. In the standard analysis, we estimated clock parameters modeled as
162 random walk processes, constant ZWD for each station, and a constant UT1-UTC
163 offset. Between the sessions, the ZWD and UT1-UTC were modeled as random
164 walk processes with Power Spectral Densities (PSD) of $58 \text{ cm}^2/\text{day}$ and $1 \text{ ms}^2/\text{day}$,
165 respectively, while the clocks were completely reset at the beginning of each ses-
166 sion.

167 2.1 GPS analysis

168 In the study, we have tested using tropospheric parameters from GPS in the data
169 analysis of the Intensives. We used GPS data from the three main Intensive sta-
170 tions: Wettzell (GPS station WTZR), Kokee (KOKB) and Tsukuba (TSKB). The
171 GPS data from these stations and from the period 2002–2015 were analyzed with

¹ http://itrf.ign.fr/ITRF_solutions/2014/

² <ftp://maia.usno.navy.mil/ser7/finals.daily>

172 GFZ's GNSS analysis software package, Earth Parameter and Orbit determination
173 System (EPOS) (Deng et al., 2016). The station parameters were estimated using
174 the precise point positioning (PPP) model. In the processing, the GPS orbits and
175 clocks were fixed to those from the 2nd IGS TIGA (Tide Gauge Benchmark Mon-
176 itoring) reprocessing and the GFZ routine IGS final products. The station-related
177 parameters were estimated based on least-squares adjustment: station positions
178 with daily resolution, receiver clocks for every epoch, zenith total delays with
179 30 min resolution, and tropospheric gradients with hourly resolution.

180 2.2 ERA-Interim gradients

181 The tropospheric gradients can also be calculated from the meteorological data
182 provided by numerical weather prediction models (NWM). In a NWM, the asym-
183 metric features of the troposphere are simulated by humidity and temperature
184 gradients, which are related to the gradients in the refractivity field. Thus, tropo-
185 spheric gradients can be estimated by slant delays obtained by ray-tracing through
186 the refractivity fields.

187 For our investigations we employ data from the meso-beta scale NWM ERA-
188 Interim reanalysis (Dee et al., 2011), which is the latest ECMWF re-analysis, at
189 the original resolution (6-hourly $1^\circ \times 1^\circ$ fields on 60 model levels). We utilize the
190 3D fields of temperature and specific humidity as well as the surface fields of pres-
191 sure and geopotential in order to calculate the 3D fields of partial pressure for dry
192 air and for water vapor, and therefore the hydrostatic and non-hydrostatic refrac-
193 tivity fields (Thayer, 1974). Following Zus et al. (2012) and Zus et al. (2014), 120
194 azimuth-dependent and azimuth-independent slant delays (the azimuthal spacing

195 is set to 30° , and the elevation angles are $\epsilon = [3\ 5\ 7\ 10\ 15\ 20\ 30\ 50\ 70\ 90]^\circ$ are
196 computed for each station by multiplying the zenith delays with the mapping fac-
197 tors (obtained by true direct mapping) for the hydrostatic and non-hydrostatic
198 component separately. Afterwards, the North-South and East-West gradient com-
199 ponents are estimated by least-squares fitting of the product of their differences
200 with the gradient mapping function (Chen and Herring, 1997).

201 2.3 Reference solution

202 To validate our results from the Intensives, we used the UT1-UTC estimates from
203 simultaneous standard 24-h VLBI sessions. These values provide an excellent ref-
204 erence since they have an accuracy of about $5\ \mu\text{s}$, which is significantly better
205 than the accuracy of the Intensives ($15\text{--}20\ \mu\text{s}$). In total, we used 1216 IVS-R1,
206 IVS-R4, and CONT sessions between 2002–2015 for this purpose, out of which
207 1088 sessions were simultaneous to an INT1. These sessions were also analyzed
208 with VieVS@GFZ, applying the same a priori modeling as for the Intensives.
209 The parameter estimation was performed with the classical least-squares module,
210 VIE.LSM. The parameter estimation was similar to what is described in Heinkel-
211 mann et al. (2014). For all EOP, we estimated offsets, and for polar motion and
212 UT1-UTC additionally rates. The UT1-UTC offsets and rates were then used to
213 calculate the reference values at the epochs of the Intensive sessions.

214 However, as normal 24-h VLBI sessions are typically not observed on weekends,
215 we need an alternative way to evaluate the results of the INT2 sessions. Comparing
216 against a combined EOP series such as the USNO finals is not a reliable metric
217 since the results from the Intensives are assimilated in these combinations and

218 therefore such series cannot be considered independent. Thus, we decided to do
219 the evaluation indirectly using the LOD, i.e. the negative time derivative of UT1-
220 UTC, since accurate LOD are available for every day from GPS. Of course, one
221 Intensive session is too short (1 h) to get reliable LOD estimates. However, we can
222 calculate an estimate of the mean LOD between two Intensives as the difference
223 between the UT1-UTC estimates divided by the time difference, similar to what
224 was done in, e.g., Böhm et al. (2010) and Teke et al. (2015). Since these LOD
225 values are directly calculated from the UT1-UTC estimates, they can be used as
226 an indirect way to evaluate the UT1-UTC accuracy. This method also has the
227 advantage that it is more or less independent of VLBI. However, it should be
228 noted that the LOD derived in this way will mostly be sensitive to the random
229 errors in the UT1-UTC estimates which are uncorrelated between two Intensive
230 sessions, while slowly varying systematic errors in UT1-UTC cannot be detected.

231 For the calculation of the LOD values from the Intensives we used all pairs
232 of Intensive sessions where the time difference between the sessions was less than
233 1.2 days, and the effects of zonal tides were removed before the calculations using
234 the model in the IERS 2010 Conventions (Petit and Luzum, 2010). In total, we
235 obtained 1752 LOD values from the INT1 sessions and 480 values for the INT2
236 sessions. As a reference to these estimates, we used the LOD from the IGS (In-
237 ternational GNSS Service) final solution (Dow et al., 2009). These LOD values
238 have an accuracy of about $10 \mu\text{s}$, which is better than what we expect from the
239 Intensives ($20\text{--}30 \mu\text{s}$). From the IGS time series, we first removed the effect of
240 zonal tides, then we calculated the mean LOD value for each period for which we
241 have calculated LOD from the Intensives. It should be noted that the obtained
242 reference LOD series might not be totally consistent with the LOD from the In-

243 tensives, e.g., due to slight differences in the handling of the LOD rate, however,
244 we expect these effects to be small and should not have any major impact on our
245 results.

246 **3 Results**

247 3.1 Kalman filter and least-squares solutions

248 We first compared the Kalman filter solution described in Sec. 2 to a solution
249 calculated with the classical least-squares (LSM) module of VieVS@GFZ, as well
250 as to a Kalman filter solution where each session was analyzed individually (i.e.,
251 without any constraints on the variability of ZWD and UT1-UTC between the ses-
252 sions). Table 1 shows the weighted mean (WM) and weighted root-mean-square
253 (WRMS) differences between the Intensive solutions and the reference solution
254 calculated from the 24-h VLBI sessions. We observe that the WRMS values are
255 lower for the Kalman filter solutions, and lowest for the solution where the vari-
256 ability is constrained between the sessions. Similar results are obtained if we look
257 at the LOD differences. The differences mostly come from Intensive sessions with
258 low sensitivity to UT1-UTC. Since the Kalman filter needs to be initialized with
259 initial values of the parameters and their variance-covariance matrix, the solu-
260 tion will be loosely constrained to these values. Applying constraints between the
261 sessions imposes further restrictions on the solution. This prevents the estimates
262 from differing too much w.r.t. the a priori values, which could happen should the
263 UT1-UTC sensitivity be low. For the LSM solution, we did not apply any absolute
264 constraints to the parameters, hence slightly larger WRMS values were obtained.

265 3.2 Multi-baseline Intensives

266 We made a test of the impact of having more than three stations observing an
267 Intensive. For this, we looked at the INT1 sessions which include Svetloe (65
268 sessions), as well as the INT3 sessions (149 sessions). We calculated a Kalman filter
269 solution where all observations including Svetloe or Ny-Ålesund were excluded
270 from these sessions, and compared the results to the original solution where these
271 stations were included. To get a reference for the INT3 sessions, we extrapolated
272 the UT1-UTC estimates from the 24-h sessions (for all other investigations in this
273 work, no extrapolation was performed, only interpolation). We find that the UT1-
274 UTC WRMS differences relative to the reference series increase when excluding
275 the extra stations: for the INT1 sessions with Svetloe from 20.6 μs to 21.2 μs , and
276 for the INT3 sessions from 29.0 μs to 30.1 μs . This indicates that the extra station
277 improves the precision of the UT1-UTC estimates, as expected, although it should
278 be noted that the changes in WRMS differences are not statistically significant
279 (based on a F-test of equal variance).

280 3.3 ZWD from GPS

281 If the ZWD could be fixed to accurate a priori values in the data analysis, the
282 number of parameters needed to be estimated would be reduced and thus the
283 precision of the solution (e.g., for UT1-UTC) would get better. The problem is to
284 obtain ZWD with high enough accuracy. One potential source is ZWDs estimated
285 from GPS. To test this possibility, we estimated the ZWDs from the data obtained
286 from the GPS receivers co-located with the Intensive VLBI stations. The data
287 analysis is described in Sec. 2.1. The obtained ZWD values were then corrected

288 for the height difference between the GPS antenna and the VLBI reference point,
289 the so-called tropospheric tie (Teke et al., 2013), and then used as a priori values
290 for the ZWD in a data analysis of the Intensives where the estimation of ZWD
291 was turned off. This, however, made the results worse. For the INT1 sessions, the
292 WRMS UT1-UTC difference relative to the results of the 24 h session increased
293 from 21.6 μs to 24.6 μs . When looking at the LOD results, similar results were
294 found. Here, we only used sessions for which we had GPS data for both stations,
295 in total 3063 sessions, resulting in 846 sessions which could be compared to the
296 reference solution, 1198 LOD values for INT1, and 371 LOD values for INT2.

297 Even though the GPS ZWDs are not accurate enough so that the ZWD could be
298 fixed to these values, it can still be possible to use these values in the data analysis
299 of the Intensives to improve the solution. One strategy is to include the GPS ZWDs
300 as additional observations instead of using them as a priori values. We also tested
301 this possibility. In the analysis, the uncertainty for the GPS ZWDs were assumed
302 to be given by their formal errors obtained from the GPS analysis. However, in
303 order to further consider the possibility that these formal errors are too optimistic,
304 we calculated solutions where we increased the uncertainties of the GPS ZWDs by
305 multiplying their formal errors by a constant factor. The results for LOD can be
306 seen in Fig. 2. We note that the agreement is improved (although the improvement
307 is not statistically significant) for the INT1 sessions when including the GPS ZWDs
308 with their formal errors multiplied by a factor larger than about 2.7. For factors
309 smaller than 2.7 the results are, however, degraded relative to the case when no
310 GPS ZWDs are included. We obtain similar results when comparing the UT1-UTC
311 estimates to those from the 24-h VLBI sessions. For the INT2 sessions, however,
312 we see practically no improvement when additionally using ZWDs from GPS, only

313 degradation. Both the results for INT1 and INT2 indicate that the GPS formal
314 error factor should be large. The reason for this might be that the formal errors
315 of the GPS ZWDs are too optimistic, although we did not expect this effect to
316 be that large. It is possible that the GPS ZWDs contain systematic errors, or
317 that systematic errors are introduced through the tropospheric ties. For most
318 Intensive sessions, the sensitivity to the ZWD is good, hence external information
319 is not really needed. Thus, if we include external ZWDs which contain systematic
320 errors, this will degrade the solution. Hence, the better results are obtained when
321 we assume large uncertainties of the GPS ZWDs. Only for problematic sessions,
322 where the sensitivity to the ZWD is degraded, do the external data assist in
323 improving the results. This is likely the reason why we only see improvements for
324 the INT1 sessions, since these generally contain fewer observations (20) than the
325 INT2 sessions (30–40), hence if a few observations are lost this has a larger impact
326 for the INT1 sessions.

327 3.4 Estimation of gradients

328 As noted by Nilsson et al. (2011), the estimation of gradients from the Intensive
329 sessions is possible, however they must be tightly constrained to their a priori
330 values to avoid getting unreliable results. It is, however, not clear exactly how
331 strong constraints should be applied. To test this, we calculated several solutions
332 where we also estimated gradients in the data analysis of the Intensives. The gra-
333 dients were modeled as being constant and were reinitialized before every session.
334 Between the different solutions, the a priori standard deviation of the gradients,
335 σ_{Grad} , was varied.

336 We first assumed the same accuracy for the a priori gradients for all stations.
337 Figure 3 shows the WRMS difference between the UT1-UTC values estimated from
338 the Intensives and those from the simultaneous 24-h VLBI session, as a function
339 of the assumed a priori gradient accuracy. Similarly, Fig. 4 shows the WRMS
340 difference between the LOD estimated from the Intensives and from IGS. We
341 can see that the WRMS difference for both UT1-UTC and LOD decreases when
342 gradients are estimated and the constraints are not too loose especially for the
343 INT2 sessions (Wettzell-Tsukuba). One reason why the INT2 sessions are affected
344 more than the INT1 sessions could be that the higher number of observations and
345 better sky coverage in INT2 enhance the sensitivity to gradients. Another reason
346 is that there are often large gradients present at the Tsukuba station (Teke et al.,
347 2013).

348 For the INT1 sessions, the optimal value for σ_{Grad} seems to be around 0.6 mm,
349 while for INT2 it is around 0.8 mm. The reduction in WRMS seen when using
350 these values, relative to not estimating gradients, is statistically significant for the
351 INT2 sessions and on the limit of being significant for the INT1 sessions (5 %
352 probability of false detection, based on an F-test). The reason why there is a
353 difference between the optimal σ_{Grad} for the INT1 and INT2 sessions is likely due
354 to the size and variability of the gradients varying between the stations. To obtain
355 the best results, it seems appropriate to use larger σ_{Grad} values for stations with
356 high variability in the gradients than for stations with low variability. Thus, we
357 estimated station-specific values. We did this by calculating several solutions where
358 only σ_{Grad} of one station was varied, while σ_{Grad} of the other stations was fixed to
359 0.5 mm. We find that the optimal values (those giving the lowest WRMS for UT1-
360 UTC and LOD differences) are 0.8 mm for Kokee and 1.0 mm for Tsukuba. For

361 Wettzell, we find different values for the two kinds of Intensive sessions: for INT1
362 0.3 mm and INT2 0.6 mm. The reason for the different results depending on the
363 type of Intensive could be that the INT2 sessions are more sensitive to gradients,
364 thus a larger value for σ_{Grad} can be used. When applying the optimized, station-
365 based σ_{Grad} values, the WRMS differences decrease slightly compared to having
366 the same values for all stations. The LOD WRMS differences are 24.1 μs for INT1
367 and 19.8 μs for INT2 when optimized station-based values are applied, compared
368 to 24.4 μs and 19.9 μs , respectively, when σ_{Grad} is the same for all stations.

369 3.5 ERA-Interim Gradients

370 One possible way of obtaining a priori tropospheric gradients is to calculate them
371 using the output of a NWM. In this work, we have tested using gradients calculated
372 from ERA-Interim (Dee et al., 2011), see Sec. 2.2 for details. If we fix the gradients
373 to these values in the data analysis of the Intensives, the WRMS of the UT1-UTC
374 difference relative to the reference solution marginally decreases from 21.8 μs to
375 21.4 μs for the INT1 sessions. When looking at the LOD difference between the
376 Intensives and IGS, we also find decreases in the WRMS differences: for the INT1
377 sessions from 26.2 μs to 25.5 μs , and from 25.4 μs to 24.4 μs for the INT2 sessions.

378 We also tested estimating gradients with a priori gradients from ERA-Interim.
379 As in Sec. 3.4, we varied the uncertainty of the a priori gradients, σ_{Grad} , from 0 mm
380 to 1.5 mm. The results for UT1-UTC and LOD are also depicted in Fig. 3 and
381 Fig. 4, respectively. We can see that the WRMS differences get smaller compared
382 to when using the simple APG model for the a priori gradients. The σ_{Grad} values
383 which give the smallest WRMS differences are 0.5 mm for the INT1 sessions and

384 0.7 mm for the INT2 sessions, i.e., 0.1 mm smaller than what was found in Sec. 3.4.
385 This is likely because ERA-Interim gradients are closer to the real gradients than
386 the APG model (which gives just a constant value per site and contains no time
387 variation), thus smaller adjustments are needed and hence tighter constraints can
388 be applied. For large σ_{Grad} values the difference between using a priori gradients
389 from APG or ERA-Interim diminishes, which is expected. When the gradients are
390 loosely constrained it is not important what a priori values are used.

391 3.6 Gradients from GPS

392 Another possibility to get a priori gradients is to use those estimated from GPS.
393 We used gradients estimated in the GPS analysis described in Sec. 2.1. When we
394 fix the gradients to those obtained from GPS, the UT1-UTC WRMS difference
395 relative to the estimates from the reference solution is 21.4 μ s, compared to 21.6 μ s
396 for the standard solution, i.e. there is no significant reduction in the WRMS (these
397 WRMS values are only calculated using the sessions for which high quality GPS
398 results are available for both stations, see Sec. 3.3).

399 As with the case of a priori ZWD from GPS, we also made tests where we
400 included the GPS gradients as additional observations in the data analysis of the
401 Intensives. Also here, the uncertainties of the GPS gradients were assumed to be
402 their formal errors multiplied by a factor, which was varied between the different
403 solutions. For σ_{Grad} of the a priori gradients we used here a large value (5 mm)
404 in order to have the gradients effectively only constrained by the GPS data. The
405 WRMS difference between the LOD from the Intensive solutions and IGS can
406 be seen in Fig. 5. We can see that the inclusion of GPS gradients makes the

407 WRMS smaller. The best results are obtained when a factor for the GPS formal
408 errors of about 2.5–3 is used, giving WRMS LOD differences of 22.9 μs for INT1
409 and 18.3 μs for INT2. The same conclusions can be drawn when comparing the
410 UT1-UTC estimates with the reference solution, where the WRMS difference is
411 20.2 μs for INT1 when a factor of 2.5 is applied. All the decreases in WRMS are
412 statistically significant. One reason, why the optimal factor is larger than 1, could
413 be that the formal errors of the GPS gradients are too optimistic, or that there
414 are systematic errors in these gradients. Furthermore, normally the GPS gradients
415 are included at two epochs: the beginning and the end of the Intensive session.
416 In the analysis, the GPS gradients are all assumed to be uncorrelated, however,
417 this is not generally true. Hence, this could also be a reason why the formal errors
418 need to be increased.

419 It is possible that there are unknown errors in the GPS estimated LOD, and
420 when these values are fixed in the PPP processing will probably result in errors in
421 the GPS gradient estimates. Thus, it could happen, that when these GPS gradients
422 are used in the analysis of the Intensives, corresponding errors in the UT1-UTC
423 estimates are introduced. Therefore, while the LOD agreement between the In-
424 tensives and GPS improves, the UT1-UTC estimates are actually degraded. An
425 indication that this partly being the case is that the agreement between the UT1-
426 UTC estimates of the Intensives and the 24-h VLBI sessions are not improving
427 as much as the LOD agreement. When GPS gradients are included as additional
428 observations and their formal errors are multiplied by a factor of 3, the agreement
429 for UT1-UTC and LOD from the INT1 sessions improves by 6.5 % and 12 % re-
430 spectively. Hence, as an additional independent test, we also compared the LOD
431 from the INT1 Intensives to the LOD estimated from the 24-h sessions. Here we

432 found that the WRMS LOD difference decreased from 29.1 μs to 27.2 μs , i.e., by
433 6.5 %, which is smaller than the decrease in the WRMS difference we obtain when
434 comparing with IGS LOD. Partly this is because that the LOD from VLBI has
435 slightly larger uncertainty than the IGS LOD (indicated by the higher WRMS
436 values), however, it cannot be excluded that partly it is because of the correlated
437 errors in GPS gradient and LOD estimates.

438 **4 Conclusions**

439 The results show that the UT1-UTC estimates are significantly impacted by the
440 troposphere, in particular the tropospheric gradients. Thus, we can improve the
441 results by using a more sophisticated modeling of the tropospheric parameters
442 in the data analysis. This can include better a priori information, including ob-
443 servations of the tropospheric parameters from other techniques, or to estimate
444 additional tropospheric parameters like gradients.

445 Including additional information on the ZWD, e.g., from GPS, typically makes
446 the agreement with the reference time series worse. If only the GPS ZWD are
447 included with a small weight in the INT1 sessions, a marginal reduction in the
448 WRMS differences (1 %) is found. The reason is that the ZWD can be well deter-
449 mined in the data analysis of modern-day Intensives, thus additional information
450 is not needed. Using external ZWD from GPS or NWM could, however, be in-
451 teresting for re-analysis of older Intensive sessions from the 80s and early 90s,
452 although it should be noted that reliable GPS data are only available from the
453 mid 90s. Since the older Intensives did not have as many observations as modern-

454 day Intensives, it is sometimes not possible to estimate the ZWD. Hence, for these
455 sessions external ZWD will be beneficial.

456 We recommended that a priori tropospheric gradients calculated from a NWM
457 are used since this improves the agreement with the reference series compared to
458 when applying simple empirical models such as APG. In fact, there is almost no
459 benefit in using an empirical gradient model compared to no gradient model at
460 all (i.e., zero a priori gradients). We have made investigations where zero a priori
461 gradients were used and found very small differences compared to when APG was
462 applied. Thus, it is important to model the temporal variations in the gradients,
463 not only the climatological mean.

464 Tropospheric gradients are typically not estimated in the data analysis of In-
465 tensive sessions, however, as demonstrated by our results this is possible when
466 appropriate constraints are applied. When estimating gradients the UT1-UTC
467 and LOD estimates are closer to the reference series, in particular for the INT2
468 sessions. Thus, we recommend that gradients should also be estimated when ana-
469 lyzing Intensive sessions, in particular the INT2 sessions.

470 We obtain a reduction in the WRMS differences to the reference series when
471 including external gradients from GPS in our analysis, confirming the results of
472 Teke et al. (2015). When estimating gradients and including the GPS gradients
473 as additional observations in the data analysis, the reduction of the WRMS dif-
474 ferences is significant. In principle, further improvements could be expected if we
475 additionally use a priori gradients from ERA-Interim. However, in our tests we
476 found no significant further changes.

477 In the future, we will also test using a priori tropospheric delays obtained from
478 ray-tracing through NWMs. The results of, for instance, Böhm et al. (2010) and

479 Nafisi et al. (2012) indicate that this can improve the results from the Intensives.
480 The advantage of using ray-tracing, especially if a high resolution NWM is used,
481 is that also non-linear horizontal variations will be modeled, not only the linear
482 ones described by the gradients. Furthermore, we will study other potential error
483 sources, such as the a priori EOP and unmodeled nonlinear station motions.

484 **Acknowledgements** We are grateful to the IVS for providing the data from the Intensive
485 sessions (Nothnagel et al., 2015), the IGS for providing the GPS data and the LOD series, and
486 Jan Douša for providing the gradients. We are also grateful to the three anonymous reviewers
487 for their comments which helped us improving the paper.

488 **References**

- 489 Böhm J, Werl B, Schuh H (2006) Troposphere mapping functions for GPS and very
490 long baseline interferometry from european centre for medium-range weather
491 forecasts operational analysis data. *J Geophys Res* 111:B02,406, DOI 10.1029/
492 2005JB003629
- 493 Böhm J, Hobiger T, Ichikawa R, Kondo T, Koyama Y, Pany A, Schuh H, Teke K
494 (2010) Asymmetric tropospheric delays from numerical weather models for UT1
495 determination from VLBI intensive sessions on the baseline Wettzell-Tsukuba.
496 *J Geodesy* 84:319–325, DOI 10.1007/s00190-010-0370-x
- 497 Böhm J, Böhm S, Nilsson T, Pany A, Plank L, Spicakova H, Teke K, Schuh
498 H (2012) The new Vienna VLBI software. In: Kenyon S, Pacino MC, Marti
499 U (eds) IAG Scientific Assembly 2009, Springer, Buenos Aires, Argentina, no.
500 136 in *International Association of Geodesy Symposia*, pp 1007–1011, DOI
501 10.1007/978-3-642-20338-1.126

- 502 Böhlm J, Urquhart L, Steigenberger P, Heinkelmann R, Nafisi V, Schuh H (2013)
503 A priori gradients in the analysis of space geodetic observations. In: Altamimi
504 Z, Collilieux X (eds) Reference Frames for Applications in Geosciences, IAG
505 Symposia, vol 138, Springer, pp 105–109, DOI 10.1007/978-3-642-32998-2_17
- 506 Chen G, Herring TA (1997) Effects of atmospheric azimuthal asymmetry on the
507 analysis of space geodetic data. *J Geophys Res* 102(B9):20,489–20,502, DOI
508 10.1029/97JB01739
- 509 Davis JL, Herring TA, Shapiro II, Rogers AEE, Elgered G (1985) Geodesy by radio
510 interferometry: Effects of atmospheric modeling errors on estimates of baseline
511 length. *Radio Sci* 20(6):1593–1607
- 512 Dee DP, Uppala SM, Simmons AJ, Berrisford P, Poli P, Kobayashi S, Andrae U,
513 Balmaseda MA, Balsamo G, Bauer P, Bechtold P, Beljaars ACM, van de Berg L,
514 Bidlot J, Bormann N, Delsol C, Dragani R, Fuentes M, Geer AJ, Haimberger L,
515 Healy SB, Hersbach H, Hólm EV, Isaksen L, Kållberg P, Köhler M, Matricardi
516 M, McNally AP, Monge-Sanz BM, Morcrette JJ, Park BK, Peubey C, de Rosnay
517 P, Tavolato C, Thépaut JN, Vitart F (2011) The ERA-Interim reanalysis: con-
518 figuration and performance of the data assimilation system. *Quarterly Journal*
519 *of the Royal Meteorological Society* 137(656):553–597, DOI 10.1002/qj.828
- 520 Deng Z, Scöne T, Gendt G (2016) Status of the TIGA tide gauge data reprocessing
521 at GFZ. In: Proceedings of the IAG Scientific Assembly, Potsdam, Germany,
522 DOI 10.1007/1345_2015_156, in press
- 523 Dow JM, Neilan RE, Rizos C (2009) The international GNSS service in a changing
524 landscape of global navigation satellite systems. *J Geodesy* 83:191–198, DOI
525 10.1007/s00190-008-0300-3

- 526 Fey AL, Gordon D, Jacobs CS, Ma C, Gaume RA, Arias EF, Bianco G, Boboltz
527 DA, Böckmann S, Bolotin S, Charlot P, Collioud A, Engelhardt G, Gipson J,
528 Gontier AM, Heinkelmann R, Kurdubov S, Lambert S, Lytvyn S, MacMillan DS,
529 Malkin Z, Nothnagel A, Ojha R, Skurikhina E, Sokolova J, Souchay J, Sovers
530 OJ, Tesmer V, Titov O, Wang G, Zharov V (2015) The second realization of
531 the international celestial reference frame by very long baseline interferometry.
532 *Astronomical J* 150(58):1–16, DOI 10.1088/0004-6256/150/2/58
- 533 Gipson J, Baver K (2016) Improvement of the IVS-INT01 sessions by source se-
534 lection: development and evaluation of the maximal source strategy. *J Geodesy*
535 90(3):287–303, DOI 10.1007/s00190-015-0873-6
- 536 Heinkelmann R, Nilsson T, Karbon M, Liu L, Lu C, Mora-Diaz JA, Parselia E,
537 Raposo-Pulido V, Soja B, Xu M, Schuh H (2014) The GFZ VLBI solution -
538 characteristics and first results. In: Behrend D, Baver KD, Armstrong K (eds)
539 *Proceedings of the Eight IVS General Meeting: VGOS: The New VLBI Network*,
540 Science Press, Shanghai, China, pp 330–334,
541 URL [ftp://ivscc.gsfc.nasa.gov/pub/general-meeting/2014/pdf/071_](ftp://ivscc.gsfc.nasa.gov/pub/general-meeting/2014/pdf/071_Heinkelmann_etal.pdf)
542 [Heinkelmann_etal.pdf](ftp://ivscc.gsfc.nasa.gov/pub/general-meeting/2014/pdf/071_Heinkelmann_etal.pdf)
- 543 Luzum B, Nothnagel A (2010) Improved UT1 predictions through low-latency
544 VLBI observations. *J Geodesy* 84:399–402, DOI 10.1007/s00190-010-0372-8
- 545 Malkin Z (2011) The impact of celestial pole offset modelling on VLBI UT1 in-
546 tensive results. *J Geodesy* 85(9):617–622, DOI 10.1007/s00190-011-0468-9
- 547 Malkin Z (2013) Impact of seasonal station motions on VLBI UT1 intensives
548 results. *J Geodesy* 87(6):505–514, DOI 10.1007/s00190-013-0624-5
- 549 Nafisi V, Madzak M, Böhm J, Ardalan AA, Schuh H (2012) Ray-traced tro-
550 pospheric delays in VLBI analysis. *Radio Sci* 47(2):RS2020, DOI 10.1029/

551 2011RS004918

552 Nilsson T, Haas R (2010) Impact of atmospheric turbulence on geodetic very
553 long baseline interferometry. *J Geophys Res* 115:B03,407, DOI 10.1029/
554 2009JB006579

555 Nilsson T, Böhm J, Schuh H (2011) Universal time from VLBI single-
556 baseline observations during CONT08. *J Geodesy* 85(7):415–423, DOI 10.1007/
557 s00190-010-0436-9

558 Nilsson T, Böhm J, Wijaya DD, Tresch A, Nafisi V, Schuh H (2013) Path delays in
559 the neutral atmosphere. In: Böhm J, Schuh H (eds) *Atmospheric Effects in Space*
560 *Geodesy*, Springer, Heidelberg, pp 73–136, DOI 10.1007/978-3-642-36932-2_3

561 Nilsson T, Soja B, Karbon M, Heinkelmann R, Liu L, Lu C, Mora-Diaz JA,
562 Raposo-Pulido V, Xu M, Schuh H (2014) Tropospheric modeling for the in-
563 tensive sessions. In: Behrend D, Baver KD, Armstrong K (eds) *Proceedings of*
564 *the Eight IVS General Meeting: VGOS: The New VLBI Network*, Science Press,
565 Shanghai, China, pp 288–292,
566 URL [ftp://ivscc.gsfc.nasa.gov/pub/general-meeting/2014/pdf/062_](ftp://ivscc.gsfc.nasa.gov/pub/general-meeting/2014/pdf/062_Nilsson_etal.pdf)
567 [Nilsson_etal.pdf](ftp://ivscc.gsfc.nasa.gov/pub/general-meeting/2014/pdf/062_Nilsson_etal.pdf)

568 Nilsson T, Soja B, Karbon M, Heinkelmann R, Schuh H (2015) Application of
569 Kalman filtering in VLBI data analysis. *Earth Planets Space* 67(136):1–9, DOI
570 10.1186/s40623-015-0307-y

571 Nothnagel A, Schnell D (2008) The impact of errors in polar motion and nutation
572 on UT1 determinations from VLBI intensive observations. *J Geodesy* 82:863–
573 869, DOI 10.1007/s00190-008-0212-2

574 Nothnagel A, et al (2015) The IVS data input to ITRF2014. *International VLBI*
575 *Service for Geodesy and Astrometry*, GFZ Data Services, DOI 10.5880/GFZ.1.

576 1.2015.002

577 Petit G, Luzum B (eds) (2010) IERS Conventions (2010). IERS Technical Note
578 36, Verlag des Bundesamts für Kartographie und Geodäsie, Frankfurt am Main,
579 Germany

580 Petrov L, Boy JP (2004) Study of the atmospheric pressure loading signal in VLBI
581 observations. *J Geophys Res* 109:B03,405, DOI 10.1029/2003JB002500

582 Robertson DS, Carter WE, Campbell J, Schuh H (1985) Daily Earth rotation
583 determinations from IRIS very long baseline interferometry. *Nature* 316:424–
584 427

585 Schuh H, Behrend D (2012) VLBI: A fascinating technique for geodesy and as-
586 trometry. *J Geodyn* 61:68–80, DOI 10.1016/j.jog.2012.07.007

587 Soja B, Nilsson T, Karbon M, Zus F, Dick G, Deng Z, Wickert J, Heinkelmann
588 R, Schuh H (2015) Tropospheric delay determination by Kalman filtering VLBI
589 data. *Earth Planets Space* 67(144):1–16, DOI 10.1186/s40623-015-0293-0

590 Teke K, Nilsson T, Böhm J, Hobiger T, Steigenberger P, Garcia-Espada S, Haas R,
591 Willis P (2013) Troposphere delays from space geodetic techniques, water vapor
592 radiometers, and numerical weather models over a series of continuous VLBI
593 campaigns. *J Geodesy* 87(10-12):981–1001, DOI 10.1007/s00190-013-0662-z

594 Teke K, Böhm J, Madzak M, Kwak Y, Steigenberger P (2015) GNSS zenith de-
595 lays and gradients in the analysis of VLBI Intensive sessions. *Adv Space Res*
596 56(8):16671676, DOI 10.1016/j.asr.2015.07.032

597 Thayer GD (1974) An improved equation for the radio refractive index of air.
598 *Radio Sci* 9(10):803–807

599 Zus F, Bender M, Deng Z, Dick G, Heise S, Shang-Guan M, Wickert J (2012) A
600 methodology to compute GPS slant total delays in a numerical weather model.

601 Radio Science 47(2), DOI 10.1029/2011RS004853, URL <http://dx.doi.org/>
602 [10.1029/2011RS004853](http://dx.doi.org/10.1029/2011RS004853), rS2018

603 Zus F, Dick G, Douša J, Heise S, Wickert J (2014) The rapid and precise com-
604 putation of GPS slant total delays and mapping factors utilizing a numerical
605 weather model. Radio Science 49(3):207–216, DOI 10.1002/2013RS005280, URL
606 <http://dx.doi.org/10.1002/2013RS005280>

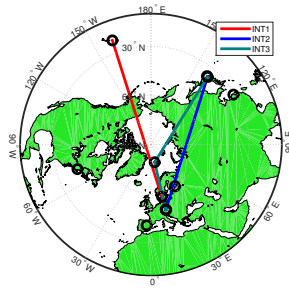


Fig. 1 Map of the stations which participated in the Intensive sessions from 2002–2015. The stations nominally participating in a particular type of Intensive sessions are connected by lines. The other stations marked with black circles are those which have participated occasionally.

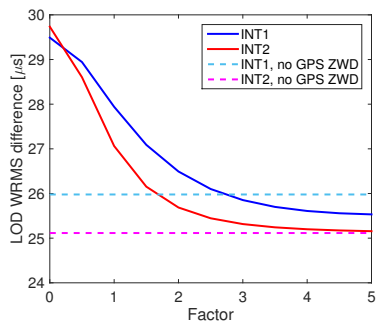


Fig. 2 WRMS difference between the LOD from the Intensives and IGS, when using ZWD from GPS as additional observations in the Kalman filter. The uncertainties of the GPS ZWDs are assumed to be their formal errors multiplied with a constant factor. Shown are the WRMS values as a function of this factor. The dashed lines show the results when no GPS ZWDs are included in the solution.

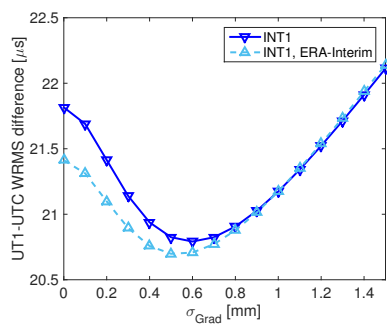


Fig. 3 WRMS differences between the UT1-UTC from the Intensives and those from the reference solution, when gradients are estimated in the data analysis. Shown are the WRMS values as a function of the assumed uncertainty of the a priori gradients, σ_{Grad} . The results from two solutions are shown, the standard one with a priori gradients from the empirical APG model (Böhm et al., 2013) and a solution with a priori gradients calculated from ERA-Interim data.

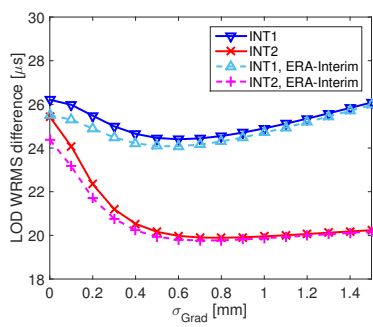


Fig. 4 Same as Fig. 3, except that here the WRMS differences between the LOD values estimated from the Intensives and those from IGS are shown.

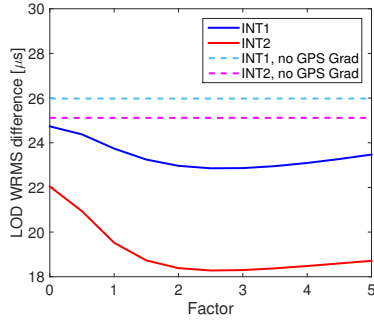


Fig. 5 WRMS difference between the LOD from the Intensives and IGS, when using gradients from GPS as additional observations in the Kalman filter. The uncertainties of the GPS gradients are assumed to be their formal errors multiplied by a constant factor. Shown are the WRMS values as function of this factor. The dashed lines show the results when no GPS gradients are included in the solution and gradients are not estimated.

Table 1 WM (WRMS) differences between the UT1-UTC estimated from the Intensive sessions and from the reference solution (simultaneous 24-h VLBI sessions). Shown are the results of one classical least-squares solution (LSM) and two Kalman filter solutions: one where all sessions are analyzed individually (KF sing), and another where loose constraints are used in between the sessions (KF cont).

Baselines	LSM [μs]	KF sing [μs]	KF cont [μs]
Wettzell–Kokee	0.4 (22.6)	0.4 (22.2)	0.5 (21.8)
Others	0.3 (21.4)	0.2 (20.8)	0.3 (20.4)
All	0.4 (22.5)	0.4 (22.0)	0.4 (21.7)